

# Response of discrete nonlinear systems with many degrees of freedom

Yaron Bromberg,<sup>1</sup> M. C. Cross,<sup>2</sup> and Ron Lifshitz<sup>1,\*</sup>

<sup>1</sup>*School of Physics and Astronomy, Raymond and Beverly Sackler*

*Faculty of Exact Sciences, Tel Aviv University, Tel Aviv 69978, Israel*

<sup>2</sup>*Department of Physics 114-36, California Institute of Technology, Pasadena, California 91125*

(Dated: October 30, 2004)

We study the response of a large array of coupled nonlinear oscillators to parametric excitation, motivated by the growing interest in the nonlinear dynamics of microelectromechanical and nanoelectromechanical systems (MEMS and NEMS). Using a multiscale analysis, we derive an amplitude equation that captures the slow dynamics of the coupled oscillators just above the onset of parametric oscillations. The amplitude equation that we derive here from first principles exhibits a wavenumber dependent bifurcation similar in character to the behavior known to exist in fluids undergoing the Faraday wave instability. We confirm this behavior numerically and make suggestions for testing it experimentally with MEMS and NEMS resonators.

PACS numbers: 85.85.+j, 05.45.-a, 45.70.Qj, 62.25.+g

In the last decade we have witnessed exciting technological advances in the fabrication and control of microelectromechanical and nanoelectromechanical systems (MEMS and NEMS). Such systems are being developed for a host of nanotechnological applications, as well as for basic research in the mesoscopic physics of phonons, and the general study of the behavior of mechanical degrees of freedom at the interface between the quantum and the classical worlds [1, 2, 3]. Surprisingly, NEMS have also opened up a new experimental window into the study of the nonlinear dynamics of discrete systems with many degrees of freedom. A combination of three properties of NEMS resonators has led to this unique experimental opportunity. First and most important is the experimental observation that micro- and nanomechanical resonators tend to behave nonlinearly at very modest amplitudes. This nonlinear behavior has not only been observed experimentally [4, 5, 6, 7, 8, 9, 10, 11], but has already been exploited to achieve mechanical signal amplification and mechanical noise squeezing [12, 13] in single resonators. Second is the fact that at their dimensions, the normal frequencies of nanomechanical resonators are extremely high—recently exceeding the 1GHz mark [14]—facilitating the design of ultra-fast mechanical devices, and making the waiting times for unwanted transients bearable on experimental time scales. Third is the technological ability to fabricate large arrays of MEMS and NEMS resonators whose collective response might be useful for signal enhancement and noise reduction [15], as well as for sophisticated mechanical signal processing applications. Such arrays have already exhibited interesting nonlinear dynamics ranging from the formation of extended patterns [16]—as one commonly observes in analogous continuous systems such as Faraday waves—to that of intrinsically localized modes [17]. Thus, nanomechanical resonator arrays are perfect for testing dynamical theories of discrete nonlinear systems with many degrees of freedom. At the same time, the the-

oretical understanding of such systems may prove useful for future nanotechnological applications.

Two of us (Lifshitz and Cross [18, henceforth LC]) have recently studied the response of coupled nonlinear oscillators to parametric excitation described by the equations

$$\begin{aligned} \ddot{u}_n + u_n + u_n^3 - \frac{1}{2}\Gamma(\dot{u}_{n+1} - 2\dot{u}_n + \dot{u}_{n-1}) \\ + \frac{1}{2}\Delta^2[1 + H \cos(2\omega_p t)](u_{n+1} - 2u_n + u_{n-1}) \\ - \frac{1}{2}\eta[(u_{n+1} - u_n)^2(\dot{u}_{n+1} - \dot{u}_n) \\ - (u_n - u_{n-1})^2(\dot{u}_n - \dot{u}_{n-1})] = 0, \end{aligned} \quad (1)$$

with  $n = 1 \dots N$ , and fixed boundary conditions  $u_0 = u_{N+1} = 0$ . We used secular perturbation theory to convert these into a set of coupled nonlinear *algebraic* equations for the normal mode amplitudes of the system, enabling us to obtain exact results for small arrays but only a qualitative understanding of the dynamics of large arrays. In order to obtain analytical results for large arrays we study here the same system of equations, approaching it from the continuous limit of infinitely-many degrees of freedom. Our central result is a scaled amplitude equation (6), governed by a single control parameter, that captures the slow dynamics of the coupled oscillators just above the onset of parametric oscillations. This amplitude equation exhibits a wavenumber-dependent bifurcation that can be traced back to the parameters of the equations of motion of the system (1). We confirm this behavior numerically and make suggestions for testing it experimentally.

The equations of motion (1) are modeled after the experiment of Buks and Roukes [16], who succeeded in fabricating, exciting, and measuring the response to parametric excitation of an array of 67 micromechanical resonating gold beams. Detailed arguments for the choice of terms introduced into the equations of motion are given by LC. The guiding principle is to introduce only those

terms that are essential for capturing the physical behavior observed in the experiment. These include a cubic nonlinear elastic restoring force (whose coefficient is scaled to 1), a dc electrostatic nearest-neighbor coupling term with a small ac component responsible for the parametric excitation (with coefficients  $\Delta^2$  and  $\Delta^2 H$  respectively), and linear as well as cubic nonlinear dissipation terms (with coefficients  $\Gamma$  and  $\eta$  respectively). The latter terms are taken to be of a nearest neighbor form, motivated by the experimental indication that most of the dissipation comes from the electrostatic interaction between neighboring beams.

The dissipation of the system is assumed to be weak, which makes it possible to excite the beams with relatively small driving amplitudes. In such case the response of the beams is moderate, justifying the description of the system with nonlinearities up to cubic terms only. The weak dissipation can be parameterized by introducing a small expansion parameter  $\epsilon \ll 1$ , physically defined by the linear dissipation coefficient  $\Gamma \equiv \epsilon\gamma$ , with  $\gamma$  of order one. The driving amplitude is then expressed by  $\Delta^2 H = \epsilon h$ , with  $h$  of order one. We assume the system is excited in its first instability tongue, i.e. we take  $\omega_p$  itself to lie within the normal frequency band  $\sqrt{1-2\Delta^2} < \omega_p < 1$ . The weakly nonlinear regime is studied by expanding the displacements  $u_n$  in powers of  $\epsilon$ . Taking the leading term to be of the order of  $\epsilon^{1/2}$  ensures that all the corrections, to a simple set of equations describing  $N$  coupled harmonic oscillators, enter the equations at the same order of  $\epsilon^{3/2}$ .

We introduce a continuous displacement field  $u(x, t)$ , keeping in mind that only for integral values  $x = n$  of the spatial coordinate does it actually correspond to the displacements  $u(n, t) = u_n(t)$  of the discrete set of oscillators in the array. We introduce slow spatial and temporal scales,  $X = \epsilon x$  and  $T = \epsilon t$ , upon which the dynamics of the envelope function occurs, and expand the displacement field in terms of  $\epsilon$ ,

$$u(x, t) = \epsilon^{1/2} [(A_+(X, T)e^{-iq_p x} + A_-^*(X, T)e^{iq_p x}) e^{i\omega_p t} + c.c.] + O(\epsilon^{3/2}), \quad (2)$$

where the asterisk and *c.c.* stand for the complex conjugate, and  $q_p$  and  $\omega_p$  are related through the dispersion relation  $\omega_p^2 = 1 - 2\Delta^2 \sin^2(q_p/2)$ . The response to lowest order in  $\epsilon$  is expressed in terms of two counter-propagating waves with complex amplitudes  $A_+$  and  $A_-$ , a typical ansatz for parametrically excited continuous systems [19], though our choice for the spatial and temporal scales, which proves useful in what follows, is not typical. Substituting (2) into the equations of motion (1) yields a solvability condition from which we can obtain

the two coupled amplitude equations,

$$\frac{\partial A_\pm}{\partial T} \pm v_g \frac{\partial A_\pm}{\partial X} = -\gamma \sin^2\left(\frac{q_p}{2}\right) A_\pm \mp i \frac{h}{2\omega_p} \sin^2\left(\frac{q_p}{2}\right) A_\mp - \left(4\eta \sin^4\left(\frac{q_p}{2}\right) \mp i \frac{3}{2\omega_p}\right) (|A_\pm|^2 + 2|A_\mp|^2) A_\pm, \quad (3)$$

where the upper signs (lower signs) give the equation for  $A_+$  ( $A_-$ ) and  $v_g = \frac{\partial \omega}{\partial q} = -\frac{\Delta^2 \sin(q_p)}{2\omega_p}$  is the group velocity. A detailed derivation of the amplitude equations (3) can be found in Ref. 20. Similar equations were previously derived for describing Faraday waves [21, 22].

By linearizing the amplitude equations (3) about the zero solution ( $A_+ = A_- = 0$ ) we find [20] that the linear combination of the two amplitudes that first becomes unstable at  $h = 2\gamma\omega_p$  is  $B \propto (A_+ - iA_-)$ —representing the emergence of a standing wave with a temporal phase of  $\pi/4$  relative to the drive—while the orthogonal linear combination of the amplitudes decays exponentially and does not participate in the dynamics at onset. Thus, just above threshold we can reduce the description of the dynamics to a single amplitude  $B$ , where at a finite amplitude above threshold a band of unstable modes around  $q_p$  can contribute to the spatial form of  $B$ . This is similar to the procedure introduced by Riecke [23] for describing the onset of Faraday waves.

We define a reduced driving amplitude  $g$  with respect to the threshold  $2\gamma\omega_p$  by letting  $(h - 2\gamma\omega_p)/2\gamma\omega_p \equiv g\delta$ , with  $\delta \ll 1$ . In order to obtain an equation, describing the relevant slow dynamics of the new amplitude  $B$ , we need to select the proper scaling of the original amplitudes  $A_\pm$ , as well as their spatial and temporal variables, with respect to the new small parameter  $\delta$ . This is achieved [20] after a process of trial and error, aided by a few heuristic arguments which we only summarize here. We assume that the coefficient of nonlinear dissipation  $\eta$  is small. It is thus apparent from the original amplitude equations (3) that a quintic term must enter in order to saturate the growth of the amplitudes  $A_\pm$ . This is similar to the situation encountered by Deissler and Brand [24] who studied localized modes near a subcritical bifurcation to traveling waves. Here this can be achieved by defining the small parameter  $\delta$  with respect to the coefficient of nonlinear dissipation—letting  $\eta = \delta^{1/2}\eta_0$ , with  $\eta_0$  of order one—and taking the amplitudes to be of order  $\delta^{1/4}$ . Further noting that with a drive amplitude that scales as  $\delta$  the growth rate scales like  $\delta$  as well, and the bandwidth of unstable wave numbers scales as  $\delta^{1/2}$ , we finally make the ansatz that

$$\begin{pmatrix} A_+ \\ A_- \end{pmatrix} = \delta^{1/4} \begin{pmatrix} 1 \\ i \end{pmatrix} B(\hat{\xi}, \hat{\tau}) + O(\delta^{3/4}), \quad (4)$$

where  $\hat{\xi} = \delta^{1/2}X$  and  $\hat{\tau} = \delta T$  are the new spatial and temporal scales respectively. The amplitude equation for  $B(\hat{\xi}, \hat{\tau})$  is derived by once again using the multiple scales

method. After applying one last set of rescaling transformations,

$$\hat{\tau} = \frac{9}{32} \frac{\tau}{\omega_p^2 \eta_0^2 \gamma \sin^{10}(q_p/2)}, \quad \hat{\xi} = \frac{3}{8} \frac{|v_g| \xi}{\omega_p \eta_0 \gamma \sin^6(q_p/2)},$$

$$|B|^2 \rightarrow \frac{16}{27} \omega_p^2 \eta_0 \gamma \sin^6\left(\frac{q_p}{2}\right) |B|^2, \quad g \rightarrow \frac{32}{9} \omega_p^2 \eta_0^2 \sin^8\left(\frac{q_p}{2}\right) g, \quad (5)$$

followed by some lengthy algebra [20], we end up with an amplitude equation governed by a single parameter,

$$\frac{\partial B}{\partial \tau} = gB + \frac{\partial^2 B}{\partial \xi^2} + i \frac{2}{3} \left( 4|B|^2 \frac{\partial B}{\partial \xi} + B^2 \frac{\partial B^*}{\partial \xi} \right) - 2|B|^2 B - |B|^4 B. \quad (6)$$

Once we have obtained this amplitude equation it can be used to study a variety of dynamical solutions, ranging from simple single-mode to more complicated nonlinear extended solutions, or possibly even localized solutions. The form of Eq. (6) is also applicable to the onset of parametrically driven standing waves in continuum systems with weak nonlinear damping, and combines in a single equation a number of effects studied previously [21, 22, 23, 24, 25, 26]. The scalings and numerical coefficients will be different in different systems. Here we focus on the regime of small reduced amplitude  $g$  and look upon the saturation of single-mode solutions of the form

$$B = b_k e^{-ik\xi}, \quad (7)$$

corresponding—via the scaling  $\hat{\xi} = S_\xi \xi$ , where the scale factor  $S_\xi$  is defined in (5)—to a standing wave with a shifted wave number  $q = q_p + k\epsilon\sqrt{\delta}/S_\xi$ . From the linear terms in the amplitude equation (6) we find, as expected, that for  $g > k^2$  the zero-displacement solution is unstable to small perturbations of the form of (7), defining the parabolic neutral stability curve, shown as a dashed line in Fig. 2. The nonlinear gradients and the cubic term take the simple form  $2(k-1)|b_k|^2 b_k$ . For  $k < 1$  these terms immediately act to saturate the growth of the amplitude assisted by the quintic term. Standing waves therefore bifurcate supercritically from the zero-displacement state. For  $k > 1$  the cubic terms act to increase the growth of the amplitude, and saturation is achieved only by the quintic term. Standing waves therefore bifurcate subcritically from the zero-displacement state. Wave-number dependent bifurcations similar in character were also predicted and observed numerically in Faraday waves [22, 25, 26]. The saturated amplitude  $|b_k|$ , obtained by setting Eq. (6) to zero, is given by

$$|b_k|^2 = (k-1) \pm \sqrt{(k-1)^2 + (g-k^2)} \geq 0. \quad (8)$$

The original boundary conditions  $u(0, t) = u(N+1, t) = 0$  impose a phase of  $\pi/4$  on  $b_k$  and require that the wave numbers be quantized  $q_m = m\pi/(N+1)$ ,  $m = 1 \dots N$ .

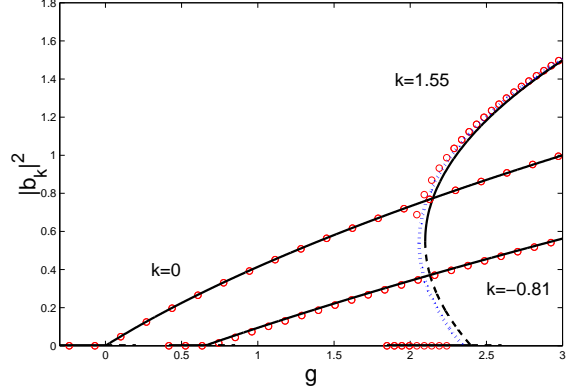


FIG. 1: (Color online) Response of the oscillator array plotted as a function of reduced amplitude  $g$  for three different wave number shifts determined by fixing the number of oscillators  $N$ :  $k = 0$  (for  $N = 100$ ) and  $k = -0.81$  (for  $N = 92$ ), which bifurcate supercritically, and  $k = 1.55$  (for  $N = 98$ ) which bifurcates subcritically showing clear hysteresis. Solid and dashed lines are the positive and negative square root branches of the calculated response in (8), the latter clearly unstable. Open circles are numerical values obtained by integration of the equations of motion (1) for each  $N$ , with  $\Delta = 0.5$ ,  $\omega_p = 0.767445$ ,  $\epsilon\gamma = 0.01$ , and  $\eta = 0.1$ . Dots show the subcritically-bifurcating single-mode solution of LC [18].

In Fig. (1) we plot  $|b_k|^2$  as a function of the reduced driving amplitude  $g$  for three different wave number shifts  $k$ . The solid (dashed) lines are the stable (unstable) solutions of Eq. (8). The circles were obtained by numerical integration of the equations of motion (1). For each driving amplitude, the Fourier components of the steady state solution were computed to verify that only single modes are found, suggesting that in this regime of parameters only these states are stable. By changing the number of oscillators  $N$  we could control the wave number shift  $k$  for a fixed value of  $\omega_p$ . In experiment it might be easier to control  $k$ , for a fixed value of  $\omega_p$ , by changing the dc component of the potential difference between the beams, thus changing the dispersion relation and with it the value of  $q_p$ .

Lifshitz and Cross [18, Eq. (33)] obtained the exact form of single mode solutions by substituting  $u_n = A_m \sin(q_m n) e^{i\omega_p t} + c.c$  directly into the equations of motion (1). In the limit of driving amplitudes just above threshold and  $\eta \ll 1$  their solution corresponds to Eq. (8), as shown by the dots in Fig. (1). In order to compare the two solutions one should note that in both cases the system oscillates in one of its normal modes  $q_m$  with the driving frequency  $\omega_p$ . Here we use  $k$  to denote the difference between  $q_p$  and the wavenumber of the oscillating pattern, whereas Lifshitz and Cross use a frequency detuning  $\omega_p - \omega_m$  to denote the difference between the normal frequency and the actual frequency of the oscillations. The frequency detuning  $\omega_p - \omega_m$  is proportional to  $v_g k \epsilon \sqrt{\delta}$ , implying that for an infinitely

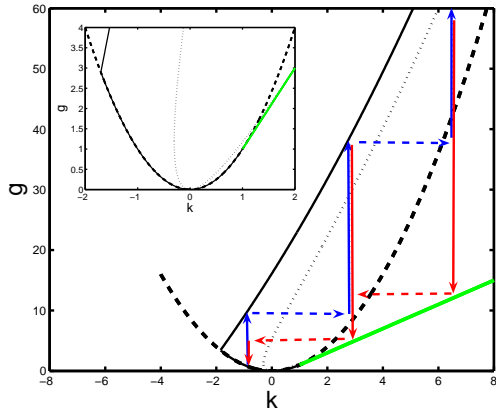


FIG. 2: (Color online) Stability boundaries of the single-mode solution of Eq. (6) in the  $g$  vs.  $k$  plane. Dashed line: neutral stability boundary. Dotted line: stability boundary of the single-mode solution (7) for a continuous spectrum. Solid line: stability boundary of the single-mode solution for  $N = 92$  and the parameters of Fig. 1. For  $k > 1$  the bifurcation from zero displacement becomes subcritical and the lower stability boundary is the locus of saddle-node bifurcations (green line). Vertical and horizontal arrows mark the secondary instability transitions shown in Fig. 3.

extended system the standing waves will always bifurcate supercritically with a wave number  $q_p$  if the driving amplitude is increased quasistatically. It is the discreteness of the normal modes which provides the detuning essential for a subcritical bifurcation if only quasistatic changes are performed.

We study secondary instabilities of the single mode solutions by performing linear stability analysis of (7). The negative square root branch in (8) is confirmed to be always unstable. The stability of the positive square root branch is bounded by the dotted curve in Fig. 2 describing the stability balloon of the single mode state. Outside the stability balloon the standing wave undergoes an Eckhaus instability with wave numbers  $k \pm Q$ , which occurs first at  $Q \rightarrow 0$ . When taking into consideration the discreteness of the system, where only wave numbers with  $Q \geq \Delta Q_N = S_\xi \pi / \epsilon \sqrt{\delta} (N+1)$  can be taken into account, the stability balloon is extended to the solid curve in the Figure, for  $N = 92$ . A transition from one single-mode state to a new single-mode state with a wave number shift of  $n\Delta Q_N$ , for some integer  $n$ , occurs once the driving amplitude is increased and has crossed the upper bound of the stability balloon. Since the upper bound monotonically increases with  $k$ , the new wave number will always be larger. A sequence of three transitions, obtained numerically, is shown in Fig. 3, superimposed with our theoretical predictions. The sequence of transitions is also sketched for comparison within the stability balloon in Fig. 2. This type of analysis yields predictions for hysteretic transitions on slow sweeps, with results for when the transition occurs and for the new state that de-

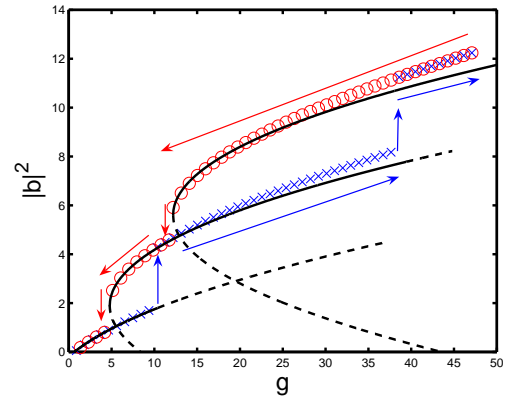


FIG. 3: (Color online) A sequence of secondary instabilities following the initial onset of single-mode oscillations in an array of 92 beams, with the parameters of Fig. 1, plotted as a function of the reduced driving amplitude  $g$ . Solid (dashed) lines are stable (unstable) solutions defined by (8), for  $k = -0.88$ ,  $k' = 2.81$ , and  $k'' = 6.51$ , corresponding to the first wave number  $k$  to emerge and two shifts to  $k + \Delta Q_N$  and  $k + 2\Delta Q_N$  respectively. Numerical integration of the equations of motion (1) for an upward sweep of  $g$  (blue  $\times$ 's), followed by a downward sweep (red  $\circ$ 's) exhibits clear hysteresis and confirms the theoretical predictions for the stability of single-mode oscillations as illustrated in Fig. 2.

velops, which for larger  $g$  must be selected out of a band of possible stable states.

We have focused here on single-mode solutions of our newly-derived amplitude equation (6) and their secondary instabilities, both of which have been numerically verified and should be experimentally tested on arrays of MEMS or NEMS resonators. In the near future we intend to study the prediction of the amplitude equations for faster ramps of the driving amplitude, including the possibility of wavenumber jumps larger than  $\Delta Q_N$  and multi-mode solutions arising from the nonlinear saturation of complex patterns growing from random initial displacements. In addition, we will investigate the behavior on slow and fast frequency sweeps.

This research is supported by the U.S.-Israel Binational Science Foundation (BSF) under Grant No. 1999458, the National Science Foundation under Grant No. DMR-0314069, and the PHYSBIO program with funds from the EU and NATO.

\* Corresponding author: ronlif@tau.ac.il

- [1] M. L. Roukes, *Scientific American* **285**, 42 (2001).
- [2] A. N. Cleland, *Foundations of Nanomechanics* (Springer, Berlin, 2003).
- [3] M. P. Blencowe, *Physics Reports* **395**, 159 (2004).
- [4] K. L. Turner, S. A. Miller, P. G. Hartwell, N. C. MacDonald, S. H. Strogatz, and S. G. Adams, *Nature* **396**, 149 (1998).

- [5] H. G. Craighead, *Science* **290**, 1532 (2000).
- [6] E. Buks and M. L. Roukes, *Europhys. Lett.* **54**, 220 (2001).
- [7] D. V. Scheible, A. Erbe, and R. H. Blick, *Appl. Phys. Lett.* **81**, 1884 (2002).
- [8] W. Zhang, R. Baskaran, and K. L. Turner, *Sensors and Actuators A* **102**, 139 (2002).
- [9] W. Zhang, R. Baskaran, and K. Turner, *Appl. Phys. Lett.* **82**, 130 (2003).
- [10] M.-F. Yu, G. J. Wagner, R. S. Ruoff, and M. J. Dyer, *Phys. Rev. B* **66**, 073406 (2002).
- [11] J. S. Aldridge and A. N. Cleland, preprint (cond-mat/0406528) (2004).
- [12] D. Rugar and P. Grütter, *Phys. Rev. Lett.* **67**, 699 (1991).
- [13] D. W. Carr, S. Evoy, L. Sekaric, H. G. Craighead, and J. M. Parpia, *Appl. Phys. Lett.* **77**, 1545 (2000).
- [14] X. M. H. Huang, C. A. Zorman, M. Mehregany, and M. L. Roukes, *Nature* **421**, 496 (2003).
- [15] M. C. Cross, A. Zumdieck, R. Lifshitz, and J. L. Rogers, *Phys. Rev. Lett.* (2004), accepted for publication (cond-mat/0406673).
- [16] E. Buks and M. L. Roukes, *J. MEMS* **11**, 802 (2002).
- [17] M. Sato, B. E. Hubbard, A. J. Sievers, B. Ilic, D. A. Czaplewski, and H. G. Craighead, *Phys. Rev. Lett.* **90**, 044102 (2003).
- [18] R. Lifshitz and M. C. Cross, *Phys. Rev. B* **67**, 134302 (2003).
- [19] M. C. Cross and P. C. Hohenberg, *Rev. Mod. Phys.* **65**, 851 (1993).
- [20] Y. Bromberg, Master's thesis, Tel Aviv University (2004).
- [21] A. B. Ezerski, M. I. Rabinovich, V. P. Reutov, and I. M. Starobinets, *Zh. Eksp. Teor. Fiz.* **91**, 2070 (1986), [Sov. Phys. JETP **64**, 1228 (1986)].
- [22] S. T. Milner, *J. Fluid Mech.* **225**, 81 (1991).
- [23] H. Riecke, *Europhys. Lett.* **11**, 213 (1990).
- [24] R. J. Deissler and H. R. Brand, *Phys. Rev. Lett.* **81**, 3856 (1998).
- [25] P. Chen and K.-A. Wu, *Phys. Rev. Lett.* **85**, 3813 (2000).
- [26] P. Chen, *Phys. Rev. E* **65**, 036308 (2002).